Neuroradiology (2020) 62:1003–1015
https://doi.org/10.1007/s00234-020-02446-4

PAEDIATRIC NEURORADIOLOGY

Spatial coefficient of variation applied to arterial spin labeling MRI may contribute to predict surgical revascularization outcomes in pediatric moyamoya vasculopathy

Domenico Tortora[1] · Camilla Scavetta[2] · Giacomo Rebella[2] · Marta Bertamino[3] · Marcello Scala[4] · Thea Giacomini[5] · Giovanni Morana[1] · Marco Pavanello[4] · Andrea Rossi[1] · Mariasavina Severino[1]

Received: 21 February 2020 / Accepted: 20 April 2020 / Published online: 15 May 2020

Abstract

Purpose In moyamoya vasculopathy, prolonged arterial transit time may increase the arterial spin labeling (ASL) signal heterogeneity, which can be quantitatively expressed by the spatial coefficient of variation of ASL-CBF (ASL-sCoV). The aim was to compare the accuracy of ASL-sCoV and ASL-CBF with dynamic susceptibility contrast (DSC)-CBF and time-to-peak (DSC-TTP) in the evaluation of perfusion changes and clinical outcome after encephalo-duro-arterio-myo-synangiosis (EDAMS) in pediatric moyamoya patients.

Methods A total of 37 children with moyamoya vasculopathy (mean age 6.31 years (1.12–15.42)) underwent ASL and DSC perfusion imaging at 3T before and up to 24 months after EDAMS. Mean DSC-CBF, mean DSC-TTP, mean ASL-CBF, and ASL-sCoV were calculated in middle cerebral artery territories. Generalized linear model analyses were used to evaluate temporal variations of postoperative perfusion changes and to compare these variations between patients developing valid pial collateralization and those without angiographic improvement. Relationship between perfusion parameters and clinical outcome after surgery was tested using multivariate regression analysis.

Results Significant reduction was observed after EDAMS for ASL-sCoV ($P = .002$; eta-squared (η^2) = 0.247) and DSC-TTP ($P < .001$; $\eta^2 = 0.415$), whereas only a trend of increase was observed for DSC-CBF and ASL-CBF, with larger discrepancy before and 6 months after surgery. At last follow-up, children developing pial collateralization showed lower absolute ASL-sCoV ($P = .002$ Cohen's d = 0.84) and DSC-TTP ($P = .027$; Cohen's d = 0.64) and higher DSC-CBF ($P = .002$; Cohen's d = − 0.55) compared with those without vascular improvement. Low preoperative and early post-surgical ASL-sCoV predicted better long-term neurological outcome ($P < .001$; ß = − 0.631).

Conclusions ASL-sCoV may contribute to predict surgical outcomes in pediatric moyamoya patients undergoing EDAMS.

Keywords Perfusion · Cerebral blood flow · Magnetic resonance · Cerebral arteries · Neurosurgical procedures

Abbreviations

ASL	Arterial spin labeling
ATT	Arterial transit time
ATA	Arterial transit artifacts
CBF	Cerebral blood flow
DSC	Dynamic susceptibility contrast
EDAMS	Encephalo-duro-arterio-myo-synangiosis
sCoV	Spatial covariance
TTP	Time to peak

Introduction

In children with moyamoya vasculopathy, indirect revascularization techniques such as encephalo-duro-arterio-myo-

Electronic supplementary material The online version of this article (https://doi.org/10.1007/s00234-020-02446-4) contains supplementary material, which is available to authorized users.

✉ Andrea Rossi
andrearossi@gaslini.org

[1] Neuroradiology Unit, IRCCS Istituto Giannina Gaslini, via Gaslini 5, 16147 Genoa, Italy

[2] Radiology Section, Department of Health Sciences (DISSAL), University of Genoa, Genoa, Italy

[3] Rehabilitation Unit, IRCCS Istituto Giannina Gaslini, Genoa, Italy

[4] Neurosurgery Unit, IRCCS Istituto Giannina Gaslini, Genoa, Italy

[5] Neuropsychiatry Unit, IRCCS Istituto Giannina Gaslini, Genoa, Italy

synangiosis (EDAMS) are used to induce the gradual formation of anastomotic vessels with the intracranial circulation, thereby eventually reducing the risk of stroke [1]. While catheter angiography is still considered the gold standard for the evaluation of post-surgical angiogenesis [2], it is an invasive technique that often requires sedation, especially in the pediatric age group. Brain MR angiography (MRA) and perfusion MR techniques are valid complementary alternatives not only for evaluating the effectiveness of surgical revascularization but also for selecting surgical candidates [3]. Indeed, dynamic susceptibility contrast (DSC) perfusion MRI has been used to evaluate cerebral hemodynamics in pediatric moyamoya patients after revascularization surgery [4, 5]; however, this technique requires the injection of gadolinium-based contrast media, which may cause concerns regarding long-standing gadolinium retention in the brain and other body organs [6]. Arterial spin labeling (ASL) MRI may overcome this issue, since it employs magnetically labeled blood water to noninvasively estimate cerebral blood flow (CBF) [7], proving to be an effective tool for brain perfusion analysis in patients with moyamoya vasculopathy treated with revascularization surgery [8, 9]. Of note, arterial transit time (ATT)—corresponding to the time the ASL bolus takes to reach the imaged voxel—is prolonged in the territories of stenotic arteries, leading to an overestimation of hypoperfusion [10]. Conversely, arterial transit artifacts (ATA), corresponding to late-arriving blood flow through pial collateral vessels, cause increased ASL signal that may lead to underestimation of hypoperfusion [11, 12]. Hence, ASL post-label delay (PLD) should be optimized to ensure that the labeled protons have reached the brain tissue at the time of acquisition [7]. An estimation of the ATT along with the CBF quantification is important to avoid quantification errors in the CBF maps. ATT measurement can be performed using specific ASL acquisition protocols such as multiple post-labeling delay techniques, which are often omitted from clinical studies as they require extra scanning time and have lower signal-to-noise ratio [13].

Recent studies showed that it is possible to indirectly estimate ATT from a single post-labeling delay ASL image using the spatial coefficient of variation (sCoV) that describes the spatial heterogeneity of CBF in a certain brain region [13, 14]. In particular, it is assumed that a normal perfusion pattern is characterized by homogeneous CBF values across gray matter voxels of the same hemisphere thus yielding a low ASL-sCoV, whereas hemodynamic alterations leading to prolonged ATT increase CBF spatial heterogeneity, thus increasing the ASL-sCoV. In the present study, we hypothesized that ASL-sCoV may reliably assess the evolution of brain perfusion after revascularization surgery in children with moyamoya vasculopathy, and that it may correlate with long-term neurological outcome. To test this hypothesis, we compared both ASL-sCoV and ASL-CBF parameters with DSC perfusion scalars (CBF and time to peak (TTP)) and MR angiography in the evaluation of hemodynamic and vascular changes after EDAMS. Additionally, we compared the predictive value of preoperative ASL and DSC parameters for estimating the clinical outcomes after surgery.

Methods and materials

Our institutional review board approved this retrospective study, and parents provided informed consent.

Patients

We retrospectively evaluated all consecutive pediatric patients with an angiographic diagnosis of moyamoya vasculopathy who underwent indirect surgical revascularization with EDAMS at our institution between 2015 and 2017. Inclusion criteria were (i) DSC and ASL sequences performed at least at four consecutive time points, viz. preoperative (time point 1), 6 months after surgery (time point 2), 12 months after surgery (time point 3), and 24 months after surgery (time point 4); (ii) good quality MR perfusion imaging, i.e., unaffected by motion artifacts; and (iii) available clinical and EEG data before and after surgical revascularization. Preoperative neurological symptoms were collected from clinical charts.

Surgical procedure

All patients underwent EDAMS in the middle cerebral artery (MCA) territories. EDAMS is a frequently applied technique of indirect cerebral revascularization for treatment of moyamoya in children [1, 15–17]. Briefly, it consists of the identification and dissection of the temporal superficial artery with its surrounding galeal and muscular cuff. Following craniotomy, the dura is opened in a cruciate fashion, preserving the middle meningeal artery branches. The dural layers are separated, and the inner avascular layer is removed. The arachnoid is widely opened with microdissection under the surgical microscope. The superficial temporal artery is subsequently sutured to the edges. The burr holes and inner table of the bone flap are trimmed to prevent kinking and compression of the superficial temporal artery on its replacement (Fig. 1).

MR images

MRI examinations were performed on a 3T MR clinical scanner (Ingenia Cx; Philips Healthcare, Best, The Netherlands) using a 32-channel head array coil. Uncooperative patients were sedated with sevoflurane via facemasks while spontaneously breathing. The brain MRI protocol included 3D T1-weighted fast-field echo

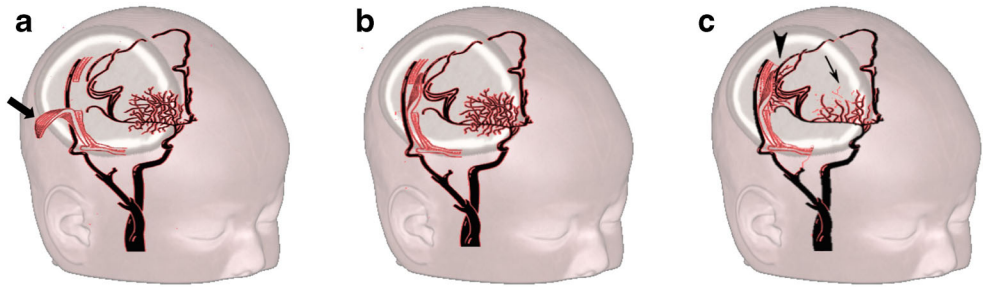

Fig. 1 Illustration of the surgical encephalo-duro-arterio-myo-synangiosis technique. **a** Identification and dissection of the temporal superficial artery with its surrounding galeal and muscular cuff (black arrow). **b** Positioning of temporal muscle on the brain surface. **c** Growth of collateral blood vessel on the pial surface of the brain after EDAMS (black arrowhead) associated with reduction of moyamoya vessels (thin black arrow)

gradient-recalled, axial 2D FLAIR, T2-weighted, and DWI sequences, and 3D TOF MR angiography. In each patient, background-suppressed pseudo-continuous arterial spin labeling (pCASL) scans with three-dimensional gradient- and spin-echo (GraSE) imaging readout module was performed using a labeling duration of 1.8 s and a PLD of 2 s. No flow-crushing gradients were applied. Label offset from the center of the imaging region was 95 mm. Other scan parameters were field of view, 256 × 160 mm; nominal voxel size, 2.0 × 2.0 × 6.0 mm^3; 22 slices; repetition time (TR)/echo time (TE), 3620 /24.78 ms; flip angle (refocusing pulses), 90°; number of segments, 1 (single-shot); and acquisition time, 4′18″. The ASL-CBF maps were generated by the MRI scanner software that was not updated during the period of patients' enrollment. For the PWI-DSC acquisition, a preload-based protocol was used. Specifically, intravenous injection of 2 mL of contrast medium (gadoterate meglumine 0.5 mmol/mL) at a flow rate of 2 mL/s, followed by a 20-mL saline flush, was routinely performed prior to perfusion-weighted imaging. After 3 min, a gradient echo EPI sequence was acquired with the following parameters: TR/TE, 2800/40 ms; flip angle, 90°; matrix, 128 × 128; FOV, 240 × 240 × 140 mm; section thickness, 5 mm; gap, 0 mm; and 28 axial sections. A series of 50 images per section was obtained before (10 images per section) and after (40 images per section) the administration of contrast agent (gadoterate meglumine 0.5 mmol/mL, 0.15 mL/kg of body weight at 3 mL/s) using a power injector (Spectris; Medrad, Pittsburgh, PA). This was followed by a 30-mL bolus of saline administered at the same injection rate. Perfusion CBF maps were computed after eliminating the effect of contrast agent recirculation by using a gamma-variate curve fitting via commercially available post-processing software (IB Neuro, Version 2.0; Imaging Biometrics, Wisconsin). Finally, post-contrast 3D T1-weighted images were obtained following DSC perfusion images.

Qualitative MRA assessment

Qualitative assessment of 3D MRA images acquired at last time point was independently performed by two pediatric neuroradiologists with 15 and 20 years of experience, blinded to perfusion analysis results. Patients were classified into two groups according to the vascular outcome, i.e., (i) improved vascularization, evidence of new pial collateral vessels after surgery and/or reduced deep collateralization; and (ii) not improved vascularization, evidence of stability or worsening of the moyamoya collateralization and absence of new pial collateral vessels. Moreover, in the 24 months 3D MRA of patients with improved vascularization, the formation of transdural collateral vessels in the middle cerebral artery territory was categorized into good, fair, and poor, considering criteria used for the angiography-based classification of Matsushima and Inaha [18]. More specifically, collateral vessels at the synangiosis site were classified as "good" if they supplied more than two-thirds of the middle cerebral artery territory, "fair" if they supplied between one-third and two-thirds, and "poor" if they supplied less than one-third [19].

Quantitative perfusion analysis

ASL-CBF, DSC-CBF, and DSC-TTP maps were co-registered with the 3D T1-weighted anatomical sequence by a linear registration process using the FMRIB Linear Image Registration Tool of FSL v.6 [20]. For quantitative analysis, an atlas-based segmentation of the MCA vascular territory was performed for each brain hemisphere, creating a single volume of interest resulting from the merger of proximal, intermediate, and distal MCA flow territory ROIs, as reported by Mutsaerts et al. [21]. Quantitative perfusion assessment was performed across the voxels of the MCA vascular territory of each hemisphere at each time point using the fslstats function of FSL, measuring the mean values and standard deviation of the three perfusion parameters, i.e., (i) ASL-CBF, (ii) DSC-CBF, (iii) and DSC-TTP. The ASL-

sCoV was then calculated at each time point as ASL-CBF standard deviation/ASL-CBF mean × 100. ASL-sCoV generates one value per ROI, with higher values indicating greater spatial heterogeneity [13]. The non-treated hemispheres of the patients who underwent unilateral revascularization were excluded from the analysis.

Clinical outcome

The neurologic outcome was evaluated based on (i) resolution or improvement of neurologic symptoms, (ii) absence of new ischemic events (transient ischemic attack and/or stroke), (iii) stability or improvement of the global intelligence quotient (IQ) score at neuropsychological evaluations, and (iv) resolution or improvement of EEG abnormalities. Patients were assigned to one of the following outcome categories by the same blinded neurologist at last follow-up: (i) excellent outcome (preoperative symptoms totally resolved without fixed neurologic deficits and EEG abnormalities, and improved global IQ score), (ii) good outcome (symptoms totally resolved with persistent EEG abnormalities and stable or improved global IQ score), (iii) fair outcome (persistent symptoms and EEG abnormalities, albeit with decreased frequency and stable or decreased global IQ score), and (iv) poor outcome (unchanged or worsened symptoms and EEG abnormalities and decreased global IQ score) [3].

Statistical analysis

Continuous variables were summarized as means and standard deviations, and categorical variables were summarized as frequencies and percentages. Wilcoxon rank and X^2 tests were used to compare continuous and categorical variables. Cohen's k coefficient has been calculated to test the interrater agreement for the qualitative assessment of MRA [22]. The generalized linear model analysis and Friedman's analysis of variance were used to test the significance of temporal variations of perfusion parameters evaluated both in the earlier and later stages after surgery. Generalized linear model analysis was also performed to evaluate differences in ASL and DSC perfusion parameters at four time points and to compare perfusion values based on the vascularization outcome. Age, gender, and the presence of bilateral moyamoya were considered as confounding factors for these analyses. Spearman's rank coefficient was used to test the correlations between perfusion parameters. In addition, agreement between ASL-CBF and DSC-CBF was also evaluated by means of the Bland-Altman method. Spearman's rank coefficient was also used to investigate and compare associations between perfusion parameters, preoperative clinical variables, and clinical outcome 24 months after surgery. Moreover, a multivariate regression analysis was performed in order to assess whether clinical and radiological parameters may predict the clinical outcome at 24 months after surgery. For this last analysis, preliminary checks were conducted to ensure that there was no violation of the independence of observations, linearity, absence of multicollinearity, homogeneity of error variances, absence of outliers, and approximal normal distribution of residuals. The level of significance was set at 0.05. All statistical analyses were performed using the SPSS Statistics software, v21 (IBM, Armonk, NY).

Results

Patients

Among 48 pediatric patients who underwent EDAMS for moyamoya vasculopathy at our institution, 37 were eligible for the study (Table 1 and Online figure 1). Bilateral revascularization in MCA territories was performed in 18 subjects and unilateral revascularization in 19. Thus, 55 surgical hemispheres (i.e., 36 from bilateral surgery and 19 from unilateral surgery) were included in the study. Overall, we analyzed 148 perfusion examinations, i.e. $n = 37$ at 4 time points.

Temporal changes of perfusion parameters after surgery

Table 2 reports mean values of ASL and DSC perfusion parameters in MCA territories at each time point. Over time, different temporal variations of CBF parameters were observed depending on the type of MR perfusion technique. In particular, a gradual and significant increase in DSC-CBF values was observed in MCA territories after surgery ($P < .001$). Conversely, only a trend of reduction was observed for ASL-CBF values 6 months after surgery followed by progressive increase of mean values from the 12th month onwards in the MCA territories ($P = .088$) (Fig. 2). Accordingly, the Bland-Altman plot analysis (Fig. 3a) revealed poor agreement between ASL-CBF and DSC-CBF in preoperative perfusion examinations (bias 9.8 mL/min/100 g; limits of agreement 23.9 and − 4.3 mL/min/100 g) with gradual improvement after surgery (from bias 3.5 mL/min/100 g at 6 months to bias − 0.6 mL/min/100 g at 24 months) (Fig. 3b–d). On the other hand, ASL-sCoV and DSC-TTP showed

Table 1 Clinical features of 37 pediatric patients with moyamoya vasculopathy

Characteristics	Value
Age at symptom onset in years (range)	6.31 ± 5.3 (1.12–15.42)
Age at first surgery in years (range)	12.63 ± 4.73 (3.11–17.92)
Interval between clinical onset and surgery in years (range)	5.27 ± 2.13 (0.5–7.76)
Females	17/37 (46%)
Moyamoya syndrome	13/37 (35%)
Clinical onset	
TIA	5/37 (13.5%)
Headache	13/37 (35.2%)
Infarction	4/37 (10.8%)
Seizure	3/37 (8%)
Hemorrhage	0/37 (-)
Asymptomatic	12/37 (32.5%)
Angiographic Suzuki stage	
1	2/37 (6%)
2	6/37 (16%)
3	9/37 (24.3%)
4	11/37 (29%)
5	8/37 (21.7%)
6	1/37 (3%)
PCA involvement	5/37 (13.5%)
Unilateral lesions	19/37 (51.3%)
Preoperative stroke	4/37 (10.8%)

similar significant progressive reduction after surgery (Fig. 4). Additionally, before surgery, DSC parameters (i.e., CBF and TTP) showed moderate-to-strong correlation only with ASL-sCoV values ($r^2 = -0.562$, $P < .001$ for DSC-CBF; $r^2 = 0.535$, $P = .001$ for DSC-TTP), while ASL-CBF correlated with DSC perfusion parameters exclusively in postoperative perfusion examinations (Fig. 5).

Table 2 Pre- and postoperative mean values and standard deviation of ASL and DSC perfusion parameters

	Time point	Mean	Standard deviation	*P*	Eta-squared
ASL-sCoV (%)	Before surgery	74.52	22.89	.003	0.247
	6 months	72.81	22.83		
	12 months	65.89	18.82		
	24 months	57.68	18.61		
ASL-CBF (mL/min/100 g)	Before surgery	28.56	5.69	.523	0.043
	6 months	26.61	7.03		
	12 months	28.66	6.08		
	24 months	28.63	6.78		
DSC-CBF (mL/min/100 g)	Before surgery	18.74	6.19	< .001	0.294
	6 months	23.07	6.56		
	12 months	27.55	9.03		
	24 months	29.61	7.43		
DSC-TTP (seconds)	Before surgery	28.35	3.88	< .001	0.415
	6 months	25.52	3.85		
	12 months	22.58	4.03		
	24 months	20.86	3.46		

P indicates statistical significance of generalized linear model analysis comparing mean values of perfusion parameters at the four time points

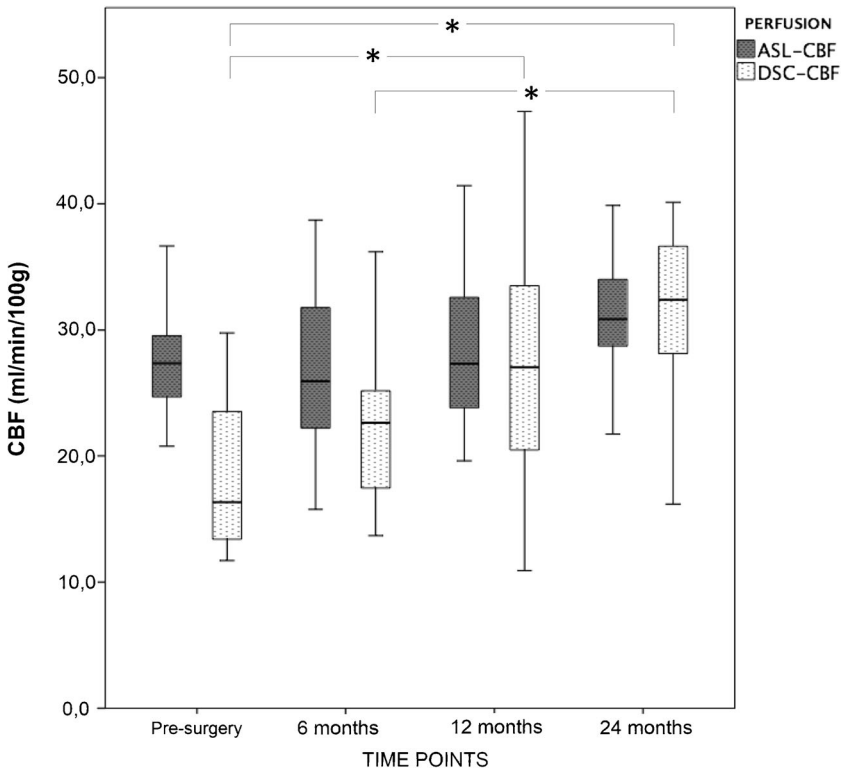

Fig. 2 Bar chart analysis revealing higher mean CBF-ASL values in the vascular territory of middle cerebral artery before surgery and in the early stages after surgery compared with DSC-CBF. Agreement between ASL-CBF and DSC-CBF improves in the later stages after surgery. Asterisks indicate adjusted $P < .001$ at post hoc analysis of Friedman's analysis of variance

Relationship between vascular collateralization and perfusion parameters

Almost perfect interrater agreement was observed for the qualitative assessment of MRA at last time point ($k = 0.982$). Based on this analysis, 24 patients showed an improved vascularization (9 male), and 13 patients revealed a not improved vascularization (5 males, mean interval after surgery 1138 ± 33 days). Moreover, in the 24 patients with improved vascularization, the degree of transdural collateral vessels development was classified as "good" in 17 patients, "fair" in 5 patients, and "poor" in 2 patients. We found significant lower ASL-sCoV and DSC-TTP, and higher DSC-CBF values after surgery in patients with improved vascularization compared with those with not improved vascularization (Table 3). Moreover, in the improved group, significant ASL-sCoV ($P = .006$) and DSC-TTP ($P < .001$) reduction and DSC-CBF ($P < .001$) improvement were observed after surgery over time (Fig. 6 and 7). In addition, in the same group of patients, we found significant correlations between the degree of collateral vessel development and the post-surgical percentage reduction of ASL-CoV ($r = -0.720$; $P < .001$; $r^2 = 0.518$) and DSC-TTP ($r = -0.482$; $P = .042$; $r^2 = 0.232$), and percentage increase of DSC-CBF ($r = 0.582$; $P = .003$; $r^2 = 0.338$).

Relation between perfusion parameters and clinical outcomes

At last follow-up, 21/37 (57%) operated children had an excellent outcome; 9/37 (24%), a good outcome; and 7/37 (19%), a fair outcome. None had a new stroke or intracranial hemorrhage during the post-surgical follow-up.

The correlation analysis revealed a significant negative correlation between the clinical outcome at 24 months, and the ASL-sCoV evaluated before revascularization ($r = -0.621$; $P < .001$). In addition, we also found a significant negative correlation between the clinical outcome and DSC-TTP values before surgery ($r = -0.301$; $P = .041$). No significant correlations were observed between preoperative DSC-CBF and ASL-CBF values and clinical outcome scores ($r = 0.258$; $P = .153$ and $r = -0.117$; $P = .492$, respectively). After surgery, lower ASL-sCoV and DSC-TTP at each time point were associated with a more favorable clinical outcome, while ASL-CBF and DSC-CBF were significantly correlated with long-term outcome only at 24-month MRI examinations (Table 4).

Analysis of preoperative clinical variables showed that a higher Suzuki stage (chi-square = 16.996, $p = .047$), preoperative infarction (chi-square = 14.405, $P = .001$), and the headache at clinical onset (chi-square = 14.339, $P < .001$) were associated with a worse long-

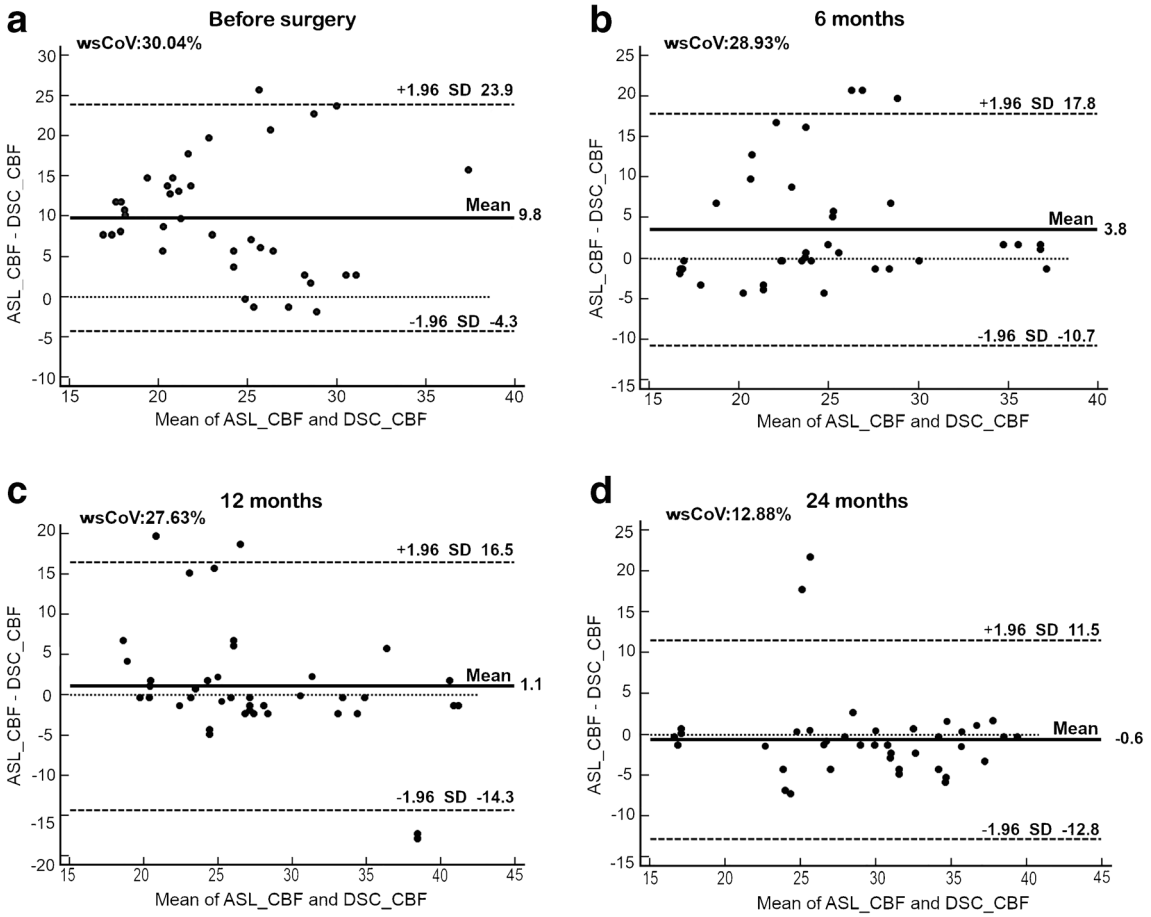

Fig. 3 Bland-Altman plots of difference between ASL-CBF and DSC-CBF values before surgery (**a**), 6 months (**b**), 12 months (**c**), and 24 months (**d**) after surgery. According to this method, a plot of the difference between ASL-CBF/DSC-CBF values (*y*-axis) against their mean (*x*-axis) was drawn and 95% limits of agreement were added to the plot (mean value ± 1.96 × standard deviation). Solid lines indicate mean absolute differences (bias); dashed lines indicate 95% limits of agreement. wsCoV is the within-subject coefficient of variation which indicates the ratio between the standard deviation of differences between ASL-CBF and DSC-CBF and the mean value of ASL-CBF and DSC-CBF. Note the lower agreement (higher bias) between ASL-CBF and DSC-CBF before surgery with gradual improvement in the later stages after surgery

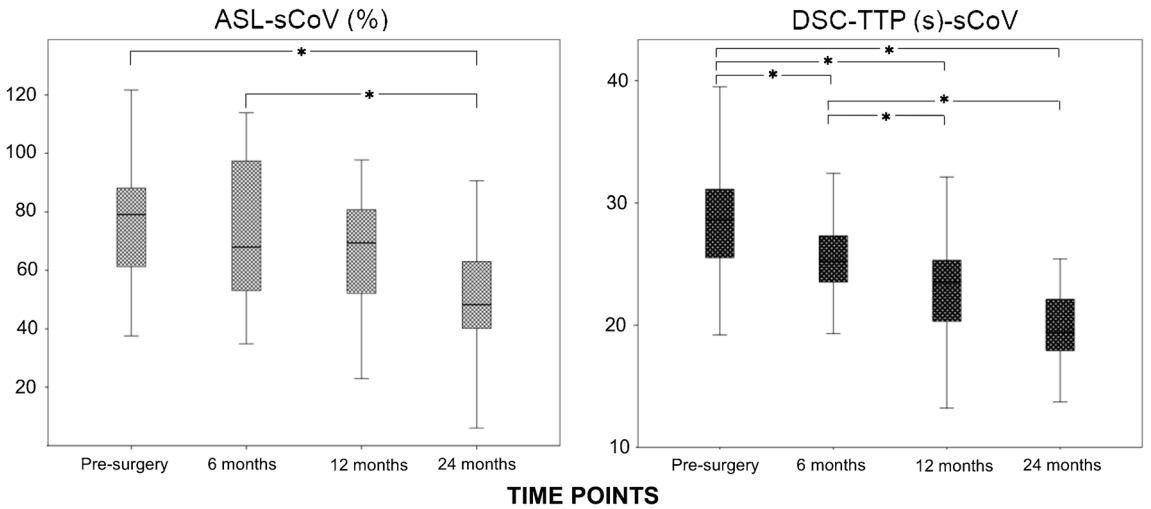

Fig. 4 Bar chart analysis revealing that ASL-sCoV and DSC-TTP showed similar significant progressive reduction after surgery in the vascular territory of middle cerebral artery. Asterisks indicate adjusted $P < .001$ at post hoc analysis of Friedman's test of variance

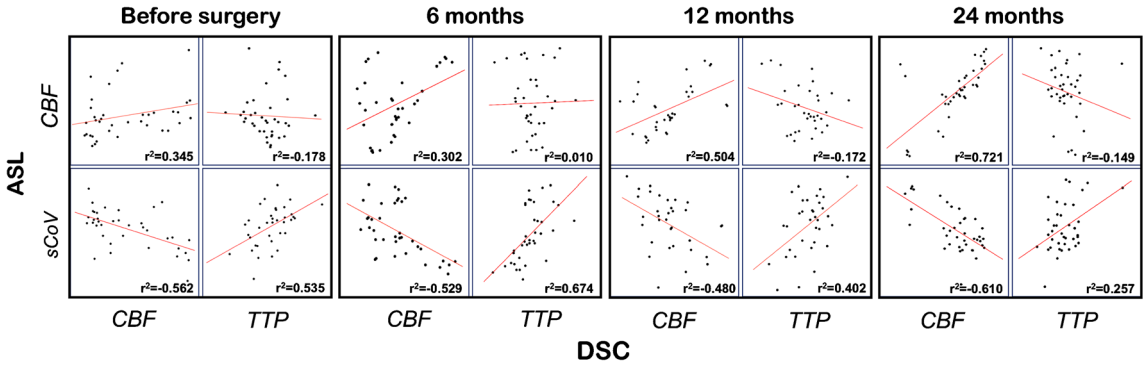

Fig. 5 Spearman's rank-order correlation analysis between ASL and DSC perfusion parameters. ASL-sCoV shows strong correlation with both DSC perfusion parameters in both pre- and postoperative perfusion examinations, while ASL-CBF correlates significantly with both DSC perfusion parameters only in postoperative perfusion time point. r^2 indicates Spearman's rank correlation coefficient

term clinical outcome. On the other hand, transient ischemic attack as initial symptom ($P = .271$), unilateral lesions ($P = .719$), and PCA involvement ($P = .118$), as well as the grade of post-surgical pial collateralization ($P = .601$) were not significantly associated with clinical outcome.

Multivariate regression analysis also demonstrated relationships between correlated factors and clinical outcomes. In particular, patients with preoperative stroke ($F = 10.684$, $P < .001$, ß = − 0.524), headache ($F = 13.370$, $P < .001$, ß = − 0.623), higher Suzuki stage ($F = 8.270$, $P = .001$, ß = − 0.558), higher ASL-sCoV before surgery ($F = 13.460$, $P < .001$, ß = − 0.631), and longer TTP 6 months after surgery ($F = 3.502$, $P = .041$, ß = − 0.405) had worst clinical outcomes. ASL-CBF and DSC-CBF values evaluated before and after surgery did not result to be significant predictors of clinical outcomes (Online-Table 1).

Discussion

This study demonstrated that spatial heterogeneity of ASL label (ASL-sCoV) in MCA vascular territory can be used to effectively evaluate brain perfusion changes in children with moyamoya vasculopathy after indirect revascularization surgery. In particular, ASL-sCoV values correlated with DSC-TTP changes, progressively decreasing after indirect revascularization surgery. Conversely, there was a discrepancy between ASL-CBF and DSC-CBF values in both preoperative and early postoperative examinations. Indeed, ASL-CBF values were higher compared with DSC-CBF values before surgery, then markedly decreased 6 months after surgery and progressively increased only in the following months. These results are in agreement with prior studies showing that quantitative analysis of ASL-CBF may be limited in moyamoya vasculopathy by several factors, including prolonged ATT leading to an underestimation of real CBF values [23–26], and ATA leading to an overestimation of CBF values in affected brain regions [25, 27]. Taken together, these factors may hamper the accuracy of regional CBF quantification with single post-label delay ASL, thus reducing the correspondence with CBF values obtained with other MR perfusion techniques. Another additional explanation for lower DSC-CBF values compared with ASL-CBF before surgery is that the former technique may be affected by the permeability of the BBB due to leaky moyamoya vessels [28]. On the other hand, we found that ASL-sCoV consistently changed accordingly to the variation of DSC-CBF and TTP, thus suggesting that this often neglected parameter may be better suited to track pre- and postoperative hemodynamic changes when using single post-label delay ASL techniques, especially in cases with moderate/severe moyamoya vasculopathy and large arterial transit artifacts. So far, ASL-sCoV has only been used in adults with cerebrovascular disease to the best of our knowledge. In particular, Mutsaerts et al. demonstrated that ASL-sCOV provides more reliable hemodynamic information about delayed arterial transit time in adults with compromised cerebral vascularization compared with ASL-CBF [13]. Moreover, Shirzadi et al. recently showed that cerebral hemodynamic alterations assessed with ASL-sCoV correlated with the clinical profiles in adults with vascular diseases and dementia, regardless of structural and metabolic abnormalities [14]. In this first pediatric study, we demonstrate that ASL-sCoV reduction reliably reflects perfusion improvement in children with moyamoya vasculopathy after EDAMS, thus representing a potential non-invasive alternative to contrast-based perfusion analyses. Nevertheless, it is important to be aware that severe moyamoya patients with very long arterial arrival time and extremely low values of ASL-CBF might show paradoxically low ASL-sCoV in the affected brain region at baseline, which may lead to erroneous interpretation of perfusion data. Similarly, patients with very mild forms of moyamoya and low preoperative ASL-sCoV values might show little variance of this parameter after surgery.

EDAMS leads to the formation of new anastomotic vessels between the external and internal arterial brain circulation,

Table 3 Mean values and standard deviation of perfusion parameters in two groups of moyamoya patients (with and without angiographic improvement)

Time point	ASL-sCoV (%)						ASL-CBF (mL/min/100 g)					
	No angiographic improvement ($N = 13$)		Angiographic improvement ($N = 24$)		P*	Cohen's d	No angiographic improvement ($N = 13$)		Angiographic improvement ($N = 24$)		P*	Cohen's d
	Mean	Standard deviation	Mean	Standard deviation			Mean	Standard deviation	Mean	Standard deviation		
Before surgery	82.91	5.71	77.32	16.89	.689	0.39	27.28	4.67	29.65	6.35	.322	− 0.41
6 months	81.62	9.98	73.43	18.41	.031	0,51	25.34	6.42	27.70	7.49	.591	− 0.33
12 months	68.32	14.41	61.29	13.72	.009	0.50	27.70	5.80	29.52	6.37	.241	− 0,29
24 months	69.42	17.81	53.81	18.89	.002	0.84	27.77	6.07	29.50	7.18	.345	− 0.26
	$P^{\dagger} = .103$		$P^{\dagger} = .006$				$P^{\dagger} = .145$		$P^{\dagger} = .225$			

Time point	DSC-CBF (mL/min/100 g)						DSC-TTP (seconds)					
	No angiographic improvement ($N = 13$)		Angiographic improvement ($N = 24$)		P*	Cohen's d	No angiographic improvement ($N = 13$)		Angiographic improvement ($N = 24$)		P*	Cohen's d
	Mean	Standard deviation	Mean	Standard deviation			Mean	Standard deviation	Mean	Standard deviation		
Before surgery	16.66	5.55	20.52	6.29	.549	− 0.64	29.62	3.41	27.27	4.01	.002	0.62
6 months	21.86	5.77	24.10	7.14	.046	− 0.33	26.46	3.35	24.71	4.15	.004	0.45
12 months	25.11	6.26	29.71	10.63	.001	− 0,49	23.80	2.62	21.49	4.79	.012	0.55
24 months	25.99	7.24	30.24	7.87	.002	− 0.55	23.10	2.05	20.62	4.53	.027	0.64
	$P^{\dagger} = .128$		$P^{\dagger} < .001$				$P^{\dagger} = .084$		$P^{\dagger} < .001$			

P* indicates statistical significance of generalized linear model analysis comparing mean values of each parameter between the two groups at each time point, after eliminating the confounding effect of age and sex. $P^{\dagger}$ indicates statistical significance of generalized linear model analysis evaluating temporal variation of perfusion parameters in each group of moyamoya patients before and after surgery

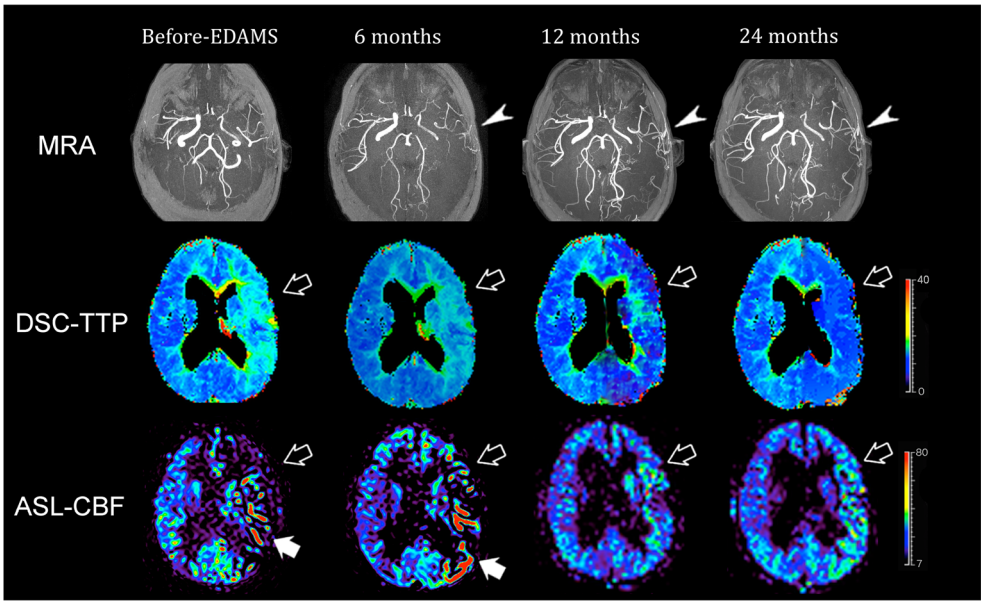

Fig. 6 Serial MR angiography and perfusion studies in a patient with left moyamoya vasculopathy treated with EDAMS. White arrowheads indicate post-surgical development of pial collateralization in the site of surgical revascularization. Progressive DSC-TTP reduction and ASL-CBF improvement occurred in the middle cerebral artery territory after surgery (empty white arrows). Note the lower spatial variation of ASL label in late post-surgical maps due to the reduction of arterial transit artifacts (white arrows) with the improvement of arterial transit time. Color bar indicates seconds and mL/min/100 g for DSC-TTP and ASL-CBF, respectively

thus supporting an adequate cerebral perfusion in patients with moyamoya vasculopathy. In the present study, we found a correlation between perfusion parameter changes and the development of pial collateralization after revascularization surgery as evaluated with MR angiography. In particular, ASL-sCoV and both DSC-related parameters changed accordingly to the degree of pial collateralization after EDAMS in subjects with improved vascularization, while no significant differences were found over time in non-improving patients. Of note, a recent study by Ha et al. demonstrated greater brain perfusion improvement in pediatric moyamoya patients developing more pial collateralization vessels after indirect

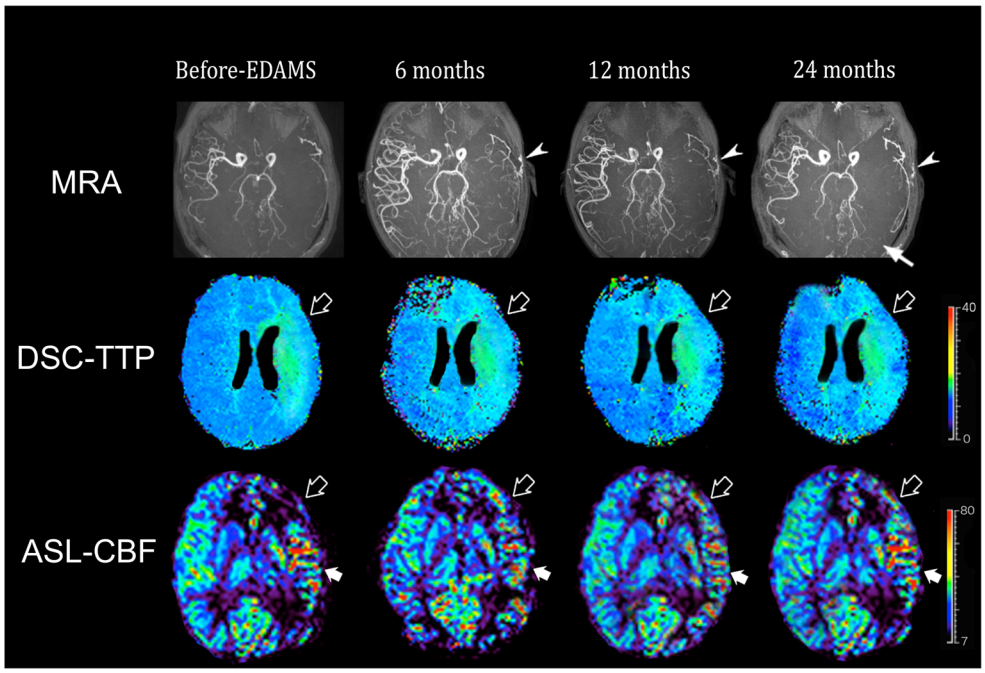

Fig. 7 Serial MR angiography and perfusion studies in a patient with left moyamoya vasculopathy treated with EDAMS and not improved vascularization after surgery. White arrowheads indicate the site of surgical revascularization. The thin white arrow indicates left parietal region with reduced number of distal branches of middle cerebral artery in the later stages after surgery. No significant improvement of DSC-TTP and ASL-CBF occurred in the middle cerebral artery territory after surgery (empty white arrows indicate high DSC-TTP and low ASL-CBF at different levels of middle cerebral artery territory). Note the high spatial variation of ASL label in pre- and post-surgical maps due to the presence of arterial transit artifacts (thick white arrows). Color bar indicates seconds and mL/min/100 g for DSC-TTP and ASL-CBF, respectively

Table 4 Correlations between perfusion parameters evaluated at each time points and long-term clinical outcome at 24 months after surgery

Perfusion Parameter	Pre-surgery		6 months		12 months		24 months	
	Rho	*P*	Rho	*P*	Rho	*P*	Rho	*P*
ASL-sCoV	−0.621	*<.001*	−0.551	*.001*	−0.487	*.003*	−0.389	*.007*
ASL-CBF	−0.117	.492	0.163	.371	0.217	.112	0.417	*.028*
DSC-CBF	0.258	.153	0.276	.202	0.228	.333	0.558	*.014*
DSC-TTP	−0.301	*.041*	−0.513	*.012*	−0.426	*.027*	−0.501	*.002*

Rho indicates Spearman's rho coefficient; *P* indicates significance level of the correlation analysis; the values reported in italics are statistically significant

revascularization as shown by catheter angiography [29]; our study came to a similar conclusion with the additional advantage of employing non-invasive MR techniques.

Furthermore, the present study found a significant correlation between clinical outcome and DSC-TTP and ASL-sCoV values, and demonstrated that beside preoperative clinical features (i.e., headache, preoperative stroke, high Suzuki stage), the evaluation of these perfusion parameters may contribute in predicting long-term clinical outcomes in pediatric patients with moyamoya. In particular, we found that higher preoperative ASL-sCoV and early post-postoperative DSC-TTP values were associated with worse clinical outcome at 24 months after surgery. On the other hand, a significant relationship was found between clinical outcome and both ASL- and DSC-CBF parameters only in the later stages after surgery. These results indicate that DSC-TTP and ASL-sCoV might be better outcome predictors compared with absolute CBF values, as the latter are highly dependent on the patient's arterial input function and may therefore underestimate perfusion in case of severe arterial stenosis [30]. We hypothesize that higher preoperative DSC-TTP and ASL-sCoV values may reflect more severe and/or advanced moyamoya vasculopathy that is less responsive to revascularization surgery in terms of formation of new pial collaterals. Indeed, Jun et al. demonstrated that the variation of TTP after revascularization surgery is the most accurate parameter for predicting clinical outcome in children with moyamoya vasculopathy, reliably reflecting collateral vessel formation after surgery [5]. Moreover, similar findings have been reported in previous studies performed in adult patients with moyamoya vasculopathy, showing that the arterial arrival time estimation, performed with both DSC and ASL perfusion techniques, may be useful for the clinical assessment of cerebral hemodynamics before and after revascularization surgery [31].

There are some limitations to our study, including its retrospective design and the relatively small cohort. Moreover, masks created for measuring perfusion parameters in the MCA territory could include subarachnoid spaces in addition to the brain parenchyma, thus affecting the accuracy of quantitative perfusion measurements. Additionally, the potential confounding effect of small head movements during the perfusion examinations and the influence of gray and white matter volume variations during the follow-up period were not controlled in the analyses, and they might influence the results of the study, masking longitudinal changes of perfusion parameters [32]. Moreover, the intrinsic low effective spatial resolution of 3DGRASE PCASL sequence may also increase the partial volume effect and influence the pial vessel depiction on ASL-CBF maps, thus potentially affecting ASL-sCoV calculation [33]. Finally, CBF-related parameters in moyamoya patients were not compared with healthy controls and with a subgroup of moyamoya patients who do not underwent EDAMS.

In conclusion, this study demonstrated that ASL-sCoV is a sensitive measure for the assessment of changes in brain perfusion after EDAMS and for the prediction of surgical outcomes in pediatric patients with moyamoya vasculopathy, thus representing a non-invasive parameter that overcomes intrinsic limitations of absolute ASL-CBF quantification. Further studies are awaited to confirm the role of ASL-sCoV in clinical practice, integrating quantitative and qualitative data, and specifically to prove the point that ASL may replace DSC MR perfusion in the assessment of children with moyamoya vasculopathy, thereby obviating the need of gadolinium-based contrast agent administration.

Acknowledgments This study was carried out within the context of the GENIUS project (Genius-GENetic Innovation to Understand Stroke "NGS per la diagnosi genetica, la terapia e il follow-up multispecialistico dei bambini con stroke") (Prot. 2017.AAI4514.U5102; ROL 20573) which was supported by the Compagnia San Paolo.

Authors' contributions - Domenico Tortora, Mariasavina Severino, and Andrea Rossi: data collection, data analysis, manuscript draft, revision of the manuscript.

- Camilla Scavetta, Giacomo Rebella, Marta Bertamino, Marcello Scala, Thea Giacomini, Giovanni Morana: data collection, images preparation, and revision of the manuscript.

Data availability Data used for the present analysis are available. For further information please write to domenicotortora@gaslini.org

Compliance with ethical standards

Conflict of interest The authors declare that they have no conflict of interest.

Ethical approval All procedures performed in the studies involving human participants were in accordance with the ethical standards of the institutional and/or national research committee and with the 1964 Helsinki Declaration and its later amendments or comparable ethical standards.

Our institutional review board (Comitato Etico Regione Liguria) approved this retrospective study.

Informed consent Informed consent was obtained from all individual participants included in the study.

Consent to participate Parents provided informed consent to participate to this study.

Consent for publication Parents provided informed consent for publication of this study.

Code availability Not applicable

References

1. Ravindran K, Wellons JC, Dewan MC (2019) Surgical outcomes for pediatric moyamoya: a systematic review and meta-analysis. J Neurosurg Pediatr 24:1–10. https://doi.org/10.3171/2019.6.PEDS19241
2. Li J, Jin M, Sun X, Li J, Liu Y, Xi Y, Wang Q, Zhao W, Huang Y (2019) Imaging of moyamoya disease and moyamoya syndrome: current status. J Comput Assist Tomogr 43:257–263. https://doi.org/10.1097/RCT.0000000000000834
3. Tortora D, Severino M, Pacetti M, Morana G, Mancardi MM, Capra V, Cama A, Pavanello M, Rossi A (2018) Noninvasive assessment of hemodynamic stress distribution after indirect revascularization for pediatric moyamoya vasculopathy. Am J Neuroradiol 39:1157–1163. https://doi.org/10.3174/ajnr.A5627
4. Calamante F, Ganesan V, Kirkham FJ, Jan W, Chong WK, Gadian DG, Connelly A (2001) MR perfusion imaging in moyamoya syndrome. Stroke 32:2810–2816. https://doi.org/10.1161/hs1201.099893
5. Yun TJ, Cheon J-E, Na DG, Kim WS, Kim IO, Chang KH, Yeon KM, Song IC, Wang KC (2009) Childhood moyamoya disease: quantitative evaluation of perfusion MR imaging—correlation with clinical outcome after revascularization surgery. Radiology 251:216–223. https://doi.org/10.1148/radiol.2511080654
6. Rossi Espagnet MC, Bernardi B, Pasquini L, Figà-Talamanca L, Tomà P, Napolitano A (2017) Signal intensity at unenhanced T1-weighted magnetic resonance in the globus pallidus and dentate nucleus after serial administrations of a macrocyclic gadolinium-based contrast agent in children. Pediatr Radiol 47:1345–1352. https://doi.org/10.1007/s00247-017-3874-1
7. Alsop DC, Detre JA, Golay X, Günther M, Hendrikse J, Hernandez-Garcia L, Lu H, MacIntosh BJ, Parkes LM, Smits M, van Osch MJP, Wang DJJ, Wong EC, Zaharchuk G (2015) Recommended implementation of arterial spin-labeled perfusion MRI for clinical applications: a consensus of the ISMRM perfusion study group and the European consortium for ASL in dementia. Magn Reson Med 73:102–116. https://doi.org/10.1002/mrm.25197
8. Saida T, Masumoto T, Nakai Y, Shiigai M, Matsumura A, Minami M (2012) Moyamoya disease: evaluation of postoperative revascularization using multiphase selective arterial spin labeling MRI. J Comput Assist Tomogr 36:143–149. https://doi.org/10.1097/RCT.0b013e31824150dd
9. Blauwblomme XT, Lemaitre XH, Naggara XO, et al Cerebral blood flow improvement after indirect revascularization for pediatric moyamoya disease: a statistical analysis of arterial spin-labeling MRI. https://doi.org/10.3174/ajnr.A4592
10. Nael K, Meshksar A, Liebeskind DS, Coull BM, Krupinski EA, Villablanca JP (2013) Quantitative analysis of hypoperfusion in acute stroke: arterial spin labeling versus dynamic susceptibility contrast. Stroke 44:3090–3096. https://doi.org/10.1161/STROKEAHA.113.002377
11. Mutsaerts HJMM, Petr J, Bokkers RPH, Lazar RM, Marshall RS, Asllani I (2020) Spatial coefficient of variation of arterial spin labeling MRI as a cerebrovascular correlate of carotid occlusive disease. PLoS One 15:e0229444. https://doi.org/10.1371/journal.pone.0229444
12. Vagal A, Aviv R, Sucharew H, Reddy M, Hou Q, Michel P, Jovin T, Tomsick T, Wintermark M, Khatri P (2018) Collateral clock is more important than time clock for tissue fate. Stroke 49:2102–2107. https://doi.org/10.1161/STROKEAHA.118.021484
13. Mutsaerts HJ, Petr J, Václavů L et al (2017) The spatial coefficient of variation in arterial spin labeling cerebral blood flow images. J Cereb Blood Flow Metab 37:3184–3192. https://doi.org/10.1177/0271678X16683690
14. Shirzadi Z, Stefanovic B, Mutsaerts HJMM, Masellis M, MacIntosh BJ, for the Alzheimer's Disease Neuroimaging Initiative (2019) Classifying cognitive impairment based on the spatial heterogeneity of cerebral blood flow images. J Magn Reson Imaging 50:858–867. https://doi.org/10.1002/jmri.26650
15. Pacetti M, Tortora D, Fiaschi P, Consales A, Piatelli G, Ravegnani M, Cama A, Pavanello M (2018) Burr holes revascularization in three pediatric cases of moyamoya syndrome: easy choice or insidious trap? Case series and review. Asian J Neurosurg 13:769–773. https://doi.org/10.4103/ajns.AJNS_155_16
16. Scala M, Fiaschi P, Capra V, Garrè ML, Tortora D, Ravegnani M, Pavanello M (2018) When and why is surgical revascularization indicated for the treatment of moyamoya syndrome in patients with RASopathies? A systematic review of the literature and a single institute experience. Childs Nerv Syst 34:1311–1323. https://doi.org/10.1007/s00381-018-3833-7
17. Tortora D, Severino M, Accogli A, Martinetti C, Vercellino N, Capra V, Rossi A, Pavanello M (2017) Moyamoya vasculopathy in PHACE syndrome: six new cases and review of the literature. World Neurosurg 108:291–302. https://doi.org/10.1016/j.wneu.2017.08.176
18. Matsushima Y, Inaba Y (1984) Moyamoya disease in children and its surgical treatment. Introduction of a new surgical procedure and its follow-up angiograms. Childs Brain 11:155–170. https://doi.org/10.1159/000120172
19. Yoon H-K, Shin H-J, Lee M, Byun HS, Na DG, Han BK (2000) MR angiography of Moyamoya disease before and after Encephaloduroarteriosynangiosis. Am J Roentgenol 174:195–200. https://doi.org/10.2214/ajr.174.1.1740195
20. Jenkinson M, Beckmann CF, Behrens TEJ, Woolrich MW, Smith SM (2012) Review FSL. Neuroimage 62:782–790. https://doi.org/10.1016/j.neuroimage.2011.09.015
21. Mutsaerts HJMM, van Dalen JW, Heijtel DFR, Groot PFC, Majoie CBLM, Petersen ET, Richard E, Nederveen AJ (2015) Cerebral perfusion measurements in elderly with hypertension using arterial spin labeling. PLoS One 10:e0133717. https://doi.org/10.1371/journal.pone.0133717
22. Cohen J (1960) A coefficient of agreement for nominal scales. Educ Psychol Meas 20:37–46. https://doi.org/10.1177/001316446002000104

23. Goetti R, O'Gorman R, Khan N, Kellenberger CJ, Scheer I (2013) Arterial spin labelling MRI for assessment of cerebral perfusion in children with moyamoya disease: comparison with dynamic susceptibility contrast MRI. Neuroradiology 55:639–647. https://doi.org/10.1007/s00234-013-1155-8
24. Wang R, Yu S, Alger JR, Zuo Z, Chen J, Wang R, An J, Wang B, Zhao J, Xue R, Wang DJJ (2014) Multi-delay arterial spin labeling perfusion MRI in moyamoya disease–comparison with CT perfusion imaging. Eur Radiol 24:1135–1144. https://doi.org/10.1007/s00330-014-3098-9
25. Sugino T, Mikami T, Miyata K, Suzuki K, Houkin K, Mikuni N (2013) Arterial spin-labeling magnetic resonance imaging after revascularization of moyamoya disease. J Stroke Cerebrovasc Dis 22:811–816. https://doi.org/10.1016/j.jstrokecerebrovasdis.2012.05.010
26. Hara S, Tanaka Y, Ueda Y, Hayashi S, Inaji M, Ishiwata K, Ishii K, Maehara T, Nariai T (2017) Noninvasive evaluation of CBF and perfusion delay of moyamoya disease using arterial spin-labeling MRI with multiple postlabeling delays: comparison with 15O-gas PET and DSC-MRI. AJNR Am J Neuroradiol 38:696–702. https://doi.org/10.3174/ajnr.A5068
27. Yoo R-E, Yun TJ, Rhim JH, Yoon BW, Kang KM, Choi SH, Kim JH, Kim JE, Kang HS, Sohn CH, Han MH (2015) Bright vessel appearance on arterial spin labeling MRI for localizing arterial occlusion in acute ischemic stroke. Stroke 46:564–567. https://doi.org/10.1161/STROKEAHA.114.007797
28. Kathuveetil A, Sylaja PN, Senthilvelan S, Chandrasekharan K, Banerjee M, Jayanand Sudhir B (2020) Vessel wall thickening and enhancement in high-resolution intracranial vessel wall imaging: a predictor of future ischemic events in moyamoya disease. Am J Neuroradiol 41:100–105. https://doi.org/10.3174/ajnr.A6360
29. Ha JY, Choi YH, Lee S, Cho YJ, Cheon JE, Kim IO, Kim WS (2019) Arterial spin labeling MRI for quantitative assessment of cerebral perfusion before and after cerebral revascularization in children with moyamoya disease. Korean J Radiol 20:985–996. https://doi.org/10.3348/kjr.2018.0651
30. Perthen JE, Calamante F, Gadian DG, Connelly A (2002) Is quantification of bolus tracking MRI reliable without deconvolution? Magn Reson Med 47:61–67. https://doi.org/10.1002/mrm.10020
31. Qiao P-G, Han C, Zuo Z-W, Wang YT, Pfeuffer J, Duan L, Qian T, Li GJ (2017) Clinical assessment of cerebral hemodynamics in moyamoya disease via multiple inversion time arterial spin labeling and dynamic susceptibility contrast-magnetic resonance imaging: a comparative study. J Neuroradiol 44:273–280. https://doi.org/10.1016/J.NEURAD.2016.12.006
32. Forkert ND, Li MD, Lober RM, Yeom KW (2016) Gray matter growth is accompanied by increasing blood flow and decreasing apparent diffusion coefficient during childhood. AJNR Am J Neuroradiol 37:1738–1744. https://doi.org/10.3174/ajnr.A4772
33. Álvarez MGM, Stobbe RW, Beaulieu C (2019) High resolution continuous arterial spin labeling of human cerebral perfusion using a separate neck tagging RF coil. PLoS One 14:e0215998. https://doi.org/10.1371/journal.pone.0215998